Electronic Supplementary Material (ESI) for Journal of Materials Chemistry A.

The vapour phase detection of explosive markers and derivatives using two fluorescent metal-organic frameworks.

Monika Jurcic,[a,b] William J. Peveler[a,b], Christopher N. Savory[c], David O. Scanlon[c,d], Anthony J. Kenyon[e] and Ivan P. Parkin[*b] .

[a] *Department of Security and Crime Science, University College London, London, WC1H 9EZ*

[b] *Department of Chemistry, University College London, London, WC1H 0AJ*

[c] *Kathleen Lonsdale Materials Chemistry, Department of Chemistry, University College London, London WC1H 0AJ*

[d] *Diamond Light Source Ltd., Diamond House, Harwell Science and Innovation Campus, Didcot, OX11 0DE*

[e] *Department of Electronic and Electrical Engineering, University College London, London, WC1H 7JE*

Supporting information

1. Full single crystal data and structure refinement

The full crystallographic data as obtained from single crystal X-ray diffraction for metal-organic framework [Zn(dcbpy)(DMF)]·DMF (**1**) is summarised in the tables below.

Empirical formula	$C_{18}H_{13}N_4O_6Zn$
Formula weight	453.75
Temperature/K	150.00(10)
Crystal system	monoclinic
Space group	$P2_1/n$
a/Å	9.3725(2)
b/Å	14.7643(3)
c/Å	14.7153(3)
α/°	90
β/°	101.058(2)
γ/°	90
Volume/Å^3	1998.47(7)
Z	4
ρ_{calc}mg/mm^3	1.508
m/mm^{-1}	2.089
F(000)	936
Crystal size/mm^3	0.06 × 0.02 × 0.001
2Θ range for data collection	8.564 to 102.878°
Index ranges	$-9 \le h \le 9$, $-14 \le k \le 14$, $-14 \le l \le 14$
Reflections collected	14313
Independent reflections	2158[R(int) = 0.0590]
Data/restraints/parameters	2158/0/282
Goodness-of-fit on F^2	1.044
Final R indexes [I>=2σ (I)]	R_1 = 0.0358, wR_2 = 0.0875
Final R indexes [all data]	R_1 = 0.0459, wR_2 = 0.0949
Largest diff. peak/hole / e Å^{-3}	0.37/-0.40

Bond Lengths for [Zn(dcbpy)(DMF)]·DMF						
Atom	Atom	Length/Å		Atom	Atom	Length/Å
Zn1	O1	2.024(2)		C2	C3	1.383(5)
Zn1	O3^1	1.973(3)		C2	C5	1.391(5)
Zn1	O5	2.100(3)		C3	C4	1.384(5)
Zn1	N1^2	2.099(3)		C5	C6	1.391(5)
Zn1	N2^2	2.173(3)		C6	C7	1.483(5)
O1	C1	1.272(5)		C7	C8	1.395(5)
O2	C1	1.233(5)		C8	C9	1.390(5)
O3	Zn1^1	1.973(3)		C9	C10	1.394(5)
O3	C12	1.281(5)		C9	C12	1.512(5)
O4	C12	1.225(5)		C10	C11	1.373(5)
O5	C13	1.226(5)		C13	N3	1.310(6)
N1	Zn1^3	2.099(3)		C15	N3	1.452(6)
N1	C4	1.339(5)		C14	N3	1.458(6)
N1	C6	1.351(5)		O6	C16	1.202(7)
N2	Zn1^3	2.173(3)		N4	C16	1.290(9)
N2	C7	1.344(5)		N4	C17	1.486(9)
N2	C11	1.343(5)		N4	C18A	1.694(16)
C1	C2	1.514(5)		N4	C18B	1.445(11)

Symmetry transformations used to generate equivalent atoms:

^{1}-X,-Y,1-Z; ^{2}-1/2+X,1/2-Y,-1/2+Z; ^{3}1/2+X,1/2-Y,1/2+Z

Table 5 Bond Angles for xstr0165.								
Atom	Atom	Atom	Angle/°		Atom	Atom	Atom	Angle/°
O1	Zn1	O5	92.41(10)		C6	C5	C2	119.7(4)
O1	Zn1	N1[1]	138.41(11)		N1	C6	C5	121.2(3)
O1	Zn1	N2[1]	87.36(11)		N1	C6	C7	115.8(3)
O3[2]	Zn1	O1	102.52(11)		C5	C6	C7	122.9(3)
O3[2]	Zn1	O5	99.14(10)		N2	C7	C6	114.5(3)
O3[2]	Zn1	N1[1]	117.87(11)		N2	C7	C8	121.9(3)
O3[2]	Zn1	N2[1]	100.92(11)		C8	C7	C6	123.6(3)
O5	Zn1	N2[1]	159.49(11)		C9	C8	C7	119.3(4)
N1[1]	Zn1	O5	90.66(11)		C8	C9	C10	118.1(4)
N1[1]	Zn1	N2[1]	76.24(12)		C8	C9	C12	122.2(3)
C1	O1	Zn1	109.7(2)		C10	C9	C12	119.7(4)
C12	O3	Zn1[2]	115.9(2)		C11	C10	C9	119.3(4)
C13	O5	Zn1	121.5(3)		N2	C11	C10	122.9(4)
C4	N1	Zn1[3]	123.3(3)		O3	C12	C9	115.5(4)
C4	N1	C6	119.0(3)		O4	C12	O3	126.0(4)
C6	N1	Zn1[3]	117.1(2)		O4	C12	C9	118.5(4)
C7	N2	Zn1[3]	115.5(2)		O5	C13	N3	126.0(4)
C11	N2	Zn1[3]	125.3(2)		C13	N3	C15	119.1(4)
C11	N2	C7	118.5(3)		C13	N3	C14	122.5(4)
O1	C1	C2	116.0(4)		C15	N3	C14	118.4(4)
O2	C1	O1	125.8(4)		C16	N4	C17	122.3(5)
O2	C1	C2	118.2(4)		C16	N4	C18A	90.2(8)
C3	C2	C1	120.9(4)		C16	N4	C18B	131.2(8)
C3	C2	C5	118.2(4)		C17	N4	C18A	137.7(7)
C5	C2	C1	120.8(3)		C18B	N4	C17	105.0(8)
C2	C3	C4	119.5(4)		O6	C16	N4	129.4(7)
N1	C4	C3	122.3(4)					

Symmetry transformations used to generate equivalent atoms:

[1]-1/2+X,1/2-Y,-1/2+Z; [2]-X,-Y,1-Z; [3]1/2+X,1/2-Y,1/2+Z

Figure S1.1 Asymmetric and extended asymmetric unit for [Zn(dcbpy)(DMF)]·DMF (**1**)

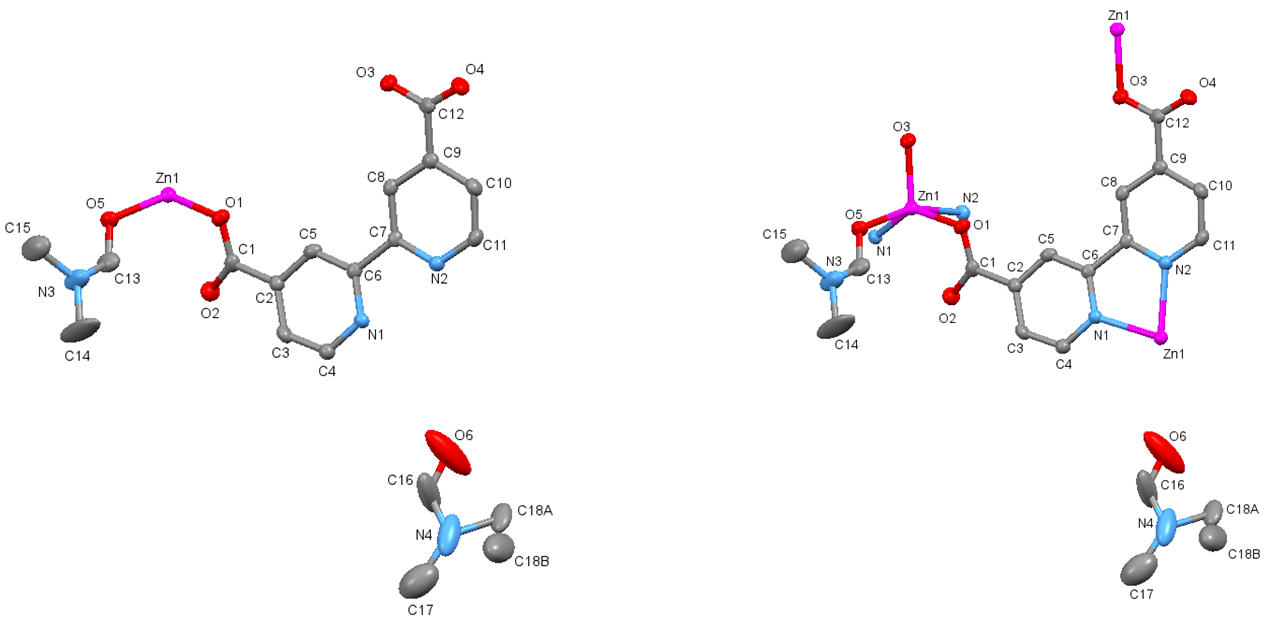

The full crystallographic data as obtained from single crystal X-ray diffraction for metal-organic framework [Dy(dcbpy)$(DMF)_2(NO_3)$] (**2**) is summarised in the tables below.

Empirical formula	$C_{18}H_{20}DyN_5O_9$
Formula weight	612.89
Temperature/K	149.90(15)
Crystal system	triclinic
Space group	P-1
a/Å	9.2414(5)
b/Å	10.3040(5)
c/Å	12.8291(6)
α/°	76.388(4)
β/°	69.431(4)
γ/°	86.377(4)
Volume/Å^3	1111.37(10)
Z	2
ρ_{calc}mg/mm^3	1.831
m/mm^{-1}	18.524
F(000)	602
Crystal size/mm^3	0.2 × 0.15 × 0.05
2Θ range for data collection	8.832 to 149.79°
Index ranges	$-11 \le h \le 11$, $-12 \le k \le 12$, $-16 \le l \le 15$
Reflections collected	16503
Independent reflections	4464[R(int) = 0.0997]
Data/restraints/parameters	4464/0/297
Goodness-of-fit on F^2	1.109
Final R indexes [I>=2σ (I)]	R_1 = 0.0576, wR_2 = 0.1489
Final R indexes [all data]	R_1 = 0.0628, wR_2 = 0.1540
Largest diff. peak/hole / e Å^{-3}	2.71/-1.63

Bond Lengths for [Dy(dcbpy)$(DMF)_2(NO_3)$]						
Atom	Atom	Length/Å		Atom	Atom	Length/Å
Dy1	O5	2.301(4)		C4	C3	1.397(8)
Dy1	O3^1	2.316(4)		C3	C2	1.391(9)
Dy1	O1	2.314(4)		N1	C13	1.309(10)
Dy1	O4	2.348(5)		N1	C15	1.456(11)
Dy1	O9	2.312(5)		N1	C14	1.415(14)
Dy1	O6	2.446(5)		C10	C10^4	1.487(12)
Dy1	O8	2.494(5)		C10	C9	1.390(8)
Dy1	N5	2.882(6)		C5	C6	1.404(10)
Dy1	O2	2.269(5)		O9	C16	1.226(9)
O5	C1^2	1.258(8)		C9	C8	1.386(8)
O3	Dy1^1	2.315(4)		N2	C16	1.300(10)
O3	C7	1.253(7)		N2	C17	1.461(11)
O1	C1	1.267(8)		N2	C18	1.426(13)
O4	C13	1.237(8)		C8	C12	1.388(9)
N4	C4	1.328(9)		C1	O5^2	1.258(8)
N4	C5	1.336(10)		C1	C2	1.505(8)
N3	C10	1.351(8)		C2	C6	1.366(10)
N3	C11	1.318(9)		C12	C11	1.395(9)
C7	C8	1.520(8)		O6	N5	1.265(9)
C7	O2	1.247(8)		O8	N5	1.240(9)
C4	C4^3	1.503(13)		N5	O7	1.247(8)

Symmetry transformations used to generate equivalent atoms:

^{1}1-X,1-Y,-Z; ^{2}1-X,-Y,-Z; ^{3}-X,-Y,1-Z; ^{4}1-X,1-Y,1-Z

Bond Angles for [Dy(dcbpy)(DMF)$_2$(NO$_3$)]								
Atom	Atom	Atom	Angle/°		Atom	Atom	Atom	Angle/°
O5	Dy1	O3^1	95.99(16)		O3	C7	C8	117.3(5)
O5	Dy1	O1	88.99(17)		O2	C7	O3	126.8(6)
O5	Dy1	O4	75.44(17)		O2	C7	C8	115.9(5)
O5	Dy1	O9	90.9(2)		N4	C4	C4^3	116.4(7)
O5	Dy1	O6	75.38(19)		N4	C4	C3	123.0(6)
O5	Dy1	O8	126.13(18)		C3	C4	C4^3	120.6(7)
O5	Dy1	N5	100.9(2)		C2	C3	C4	118.4(6)
O3^1	Dy1	O4	72.13(17)		C13	N1	C15	120.5(9)
O3^1	Dy1	O6	71.89(16)		C13	N1	C14	120.9(8)
O3^1	Dy1	O8	75.44(16)		C14	N1	C15	118.6(8)
O3^1	Dy1	N5	72.88(16)		N3	C10	C10^4	116.6(6)
O1	Dy1	O3^1	141.66(16)		N3	C10	C9	122.4(5)
O1	Dy1	O4	145.02(18)		C9	C10	C10^4	121.1(6)
O1	Dy1	O6	72.73(18)		N4	C5	C6	123.6(7)
O1	Dy1	O8	71.11(17)		C16	O9	Dy1	157.6(6)
O1	Dy1	N5	68.85(18)		C8	C9	C10	119.0(5)
O4	Dy1	O6	130.24(19)		O4	C13	N1	123.9(8)
O4	Dy1	O8	142.84(17)		C16	N2	C17	122.9(7)
O4	Dy1	N5	144.17(19)		C16	N2	C18	120.5(8)
O9	Dy1	O3^1	143.74(18)		C18	N2	C17	116.4(8)
O9	Dy1	O1	73.8(2)		C9	C8	C7	120.1(5)
O9	Dy1	O4	75.3(2)		C9	C8	C12	119.1(6)
O9	Dy1	O6	143.87(19)		C12	C8	C7	120.8(5)
O9	Dy1	O8	127.1(2)		O5^2	C1	O1	125.2(5)
O9	Dy1	N5	140.4(2)		O5^2	C1	C2	117.1(5)
O6	Dy1	O8	51.2(2)		O1	C1	C2	117.7(5)
O6	Dy1	N5	25.8(2)		C3	C2	C1	120.3(5)
O8	Dy1	N5	25.4(2)		C6	C2	C3	119.4(6)
O2	Dy1	O5	161.92(19)		C6	C2	C1	120.2(6)
O2	Dy1	O3^1	88.64(17)		C8	C12	C11	117.3(6)
O2	Dy1	O1	98.21(18)		N3	C11	C12	124.8(6)
O2	Dy1	O4	89.49(18)		O9	C16	N2	125.5(8)
O2	Dy1	O9	75.4(2)		C2	C6	C5	117.9(7)
O2	Dy1	O6	122.57(19)		N5	O6	Dy1	96.7(4)
O2	Dy1	O8	71.95(19)		N5	O8	Dy1	95.1(4)
O2	Dy1	N5	97.2(2)		O6	N5	Dy1	57.4(3)
C1^2	O5	Dy1	142.2(4)		O8	N5	Dy1	59.5(3)
C7	O3	Dy1^1	132.1(4)		O8	N5	O6	116.8(6)
C1	O1	Dy1	142.0(4)		O8	N5	O7	122.8(9)
C13	O4	Dy1	138.5(6)		O7	N5	Dy1	176.2(7)
C4	N4	C5	117.6(6)		O7	N5	O6	120.4(9)
C11	N3	C10	117.3(5)		C7	O2	Dy1	158.6(4)

Symmetry transformations used to generate equivalent atoms:

^{1}1-X,1-Y,-Z; ^{2}1-X,-Y,-Z; ^{3}-X,-Y,1-Z; ^{4}1-X,1-Y,1-Z

Figure S1.2 Asymmetric and extended asymmetric unit for [Dy(dcbpy)$(DMF)_2(NO_3)$] (**2**)

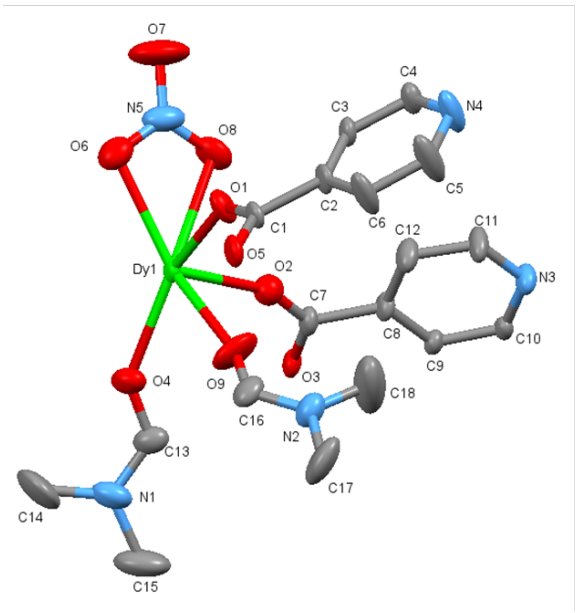

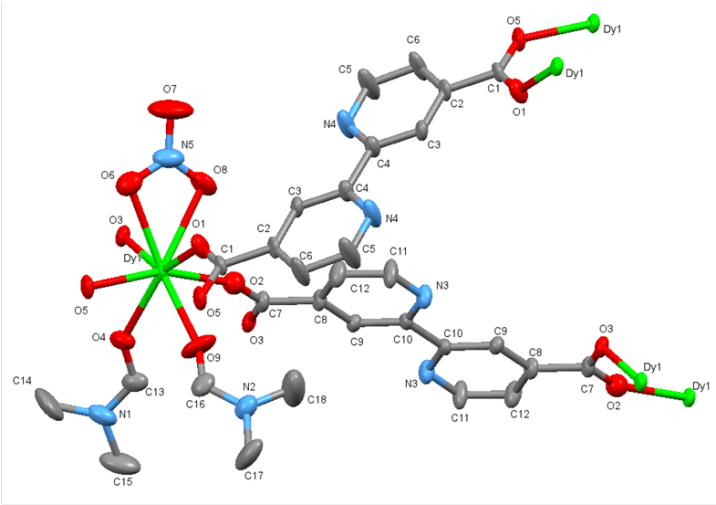

2. Space filling diagrams

Figure **S2.1** shows the space filling diagrams of MOF **1** with views along the crystallographic a) *a*-axis, b) *b*-axis and c) *c*-axis.

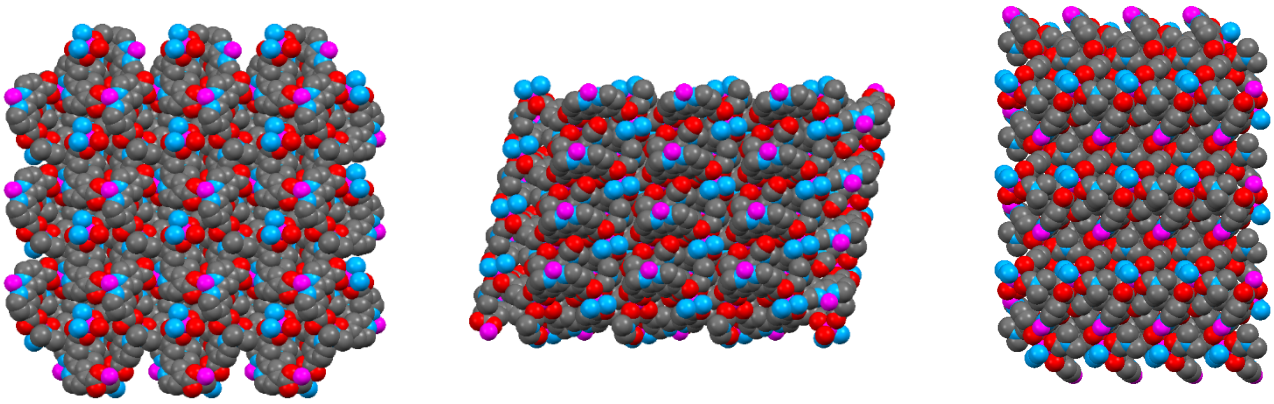

a b c

Figure **S2.2** shows the space filling diagrams of MOF **1'** with views along the crystallographic a) *a*-axis, b) *b*-axis and c) *c*-axis.

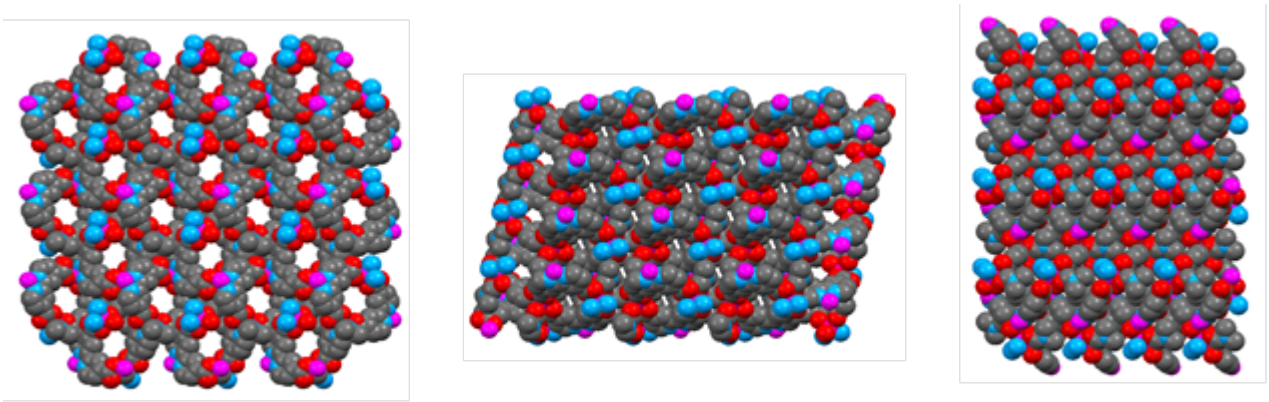

a b c

Figure **S2.3** shows the space filling diagrams of MOF **2** with views along the crystallographic a) *a*-axis, b) *b*-axis and c) *c*-axis.

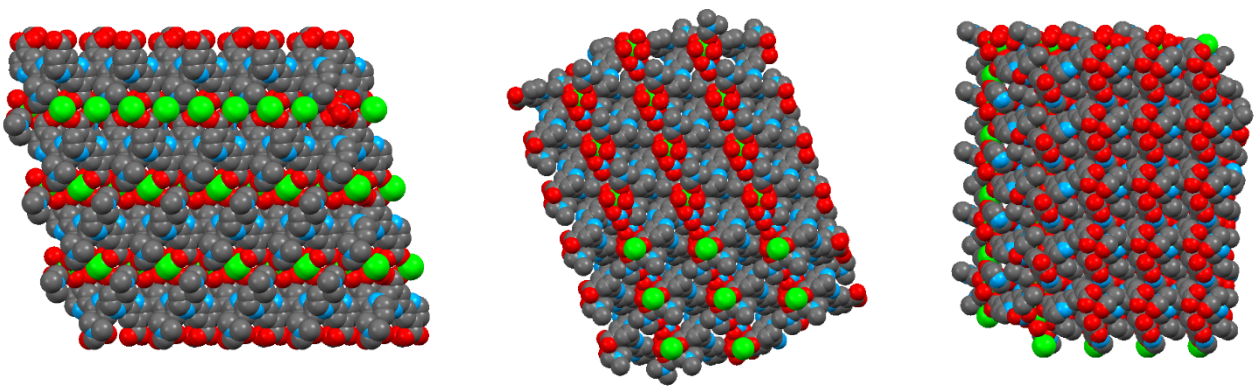

a b c

3. Scanning electron microscopy and other images

Figure S3.1 – Scanning electron microscopy image of MOF **2**

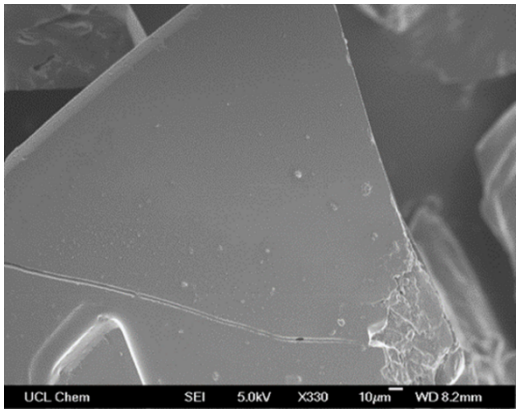

Figure S3.2 – An SEM of a typical MOF **1'** thin film

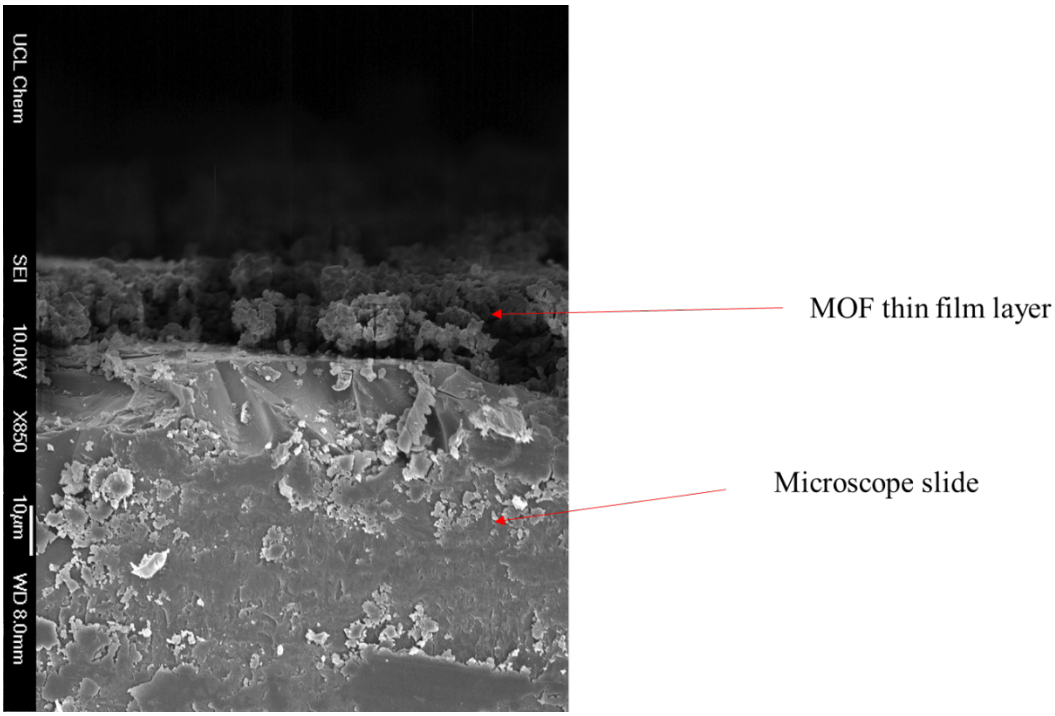

Figure S3.3 – Image of the resultant **1M** microcrystals post microwave synthesis

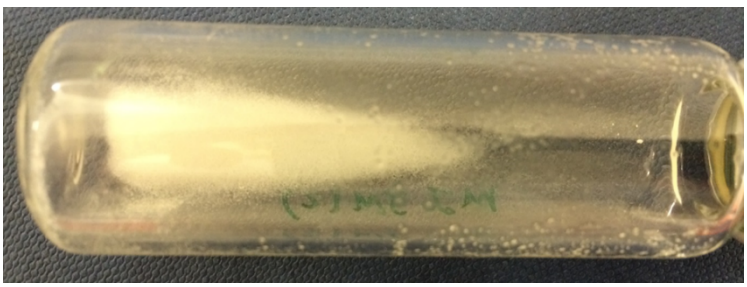

4. Thermogravimetric analysis graphs

Figure **S4.1** gives the results obtained from thermogravimetric analysis on MOF **1'**.

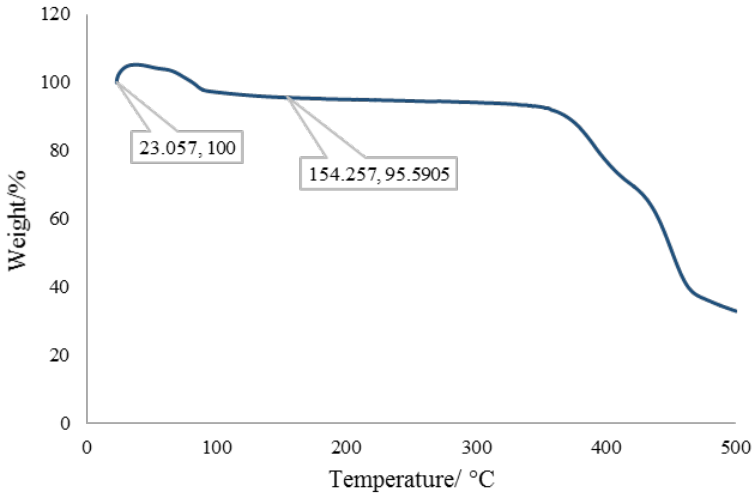

S3 – TGA results obtained for MOF **1'**.

Figure S4.2 - Thermogravimetric results of MOF **2'**.

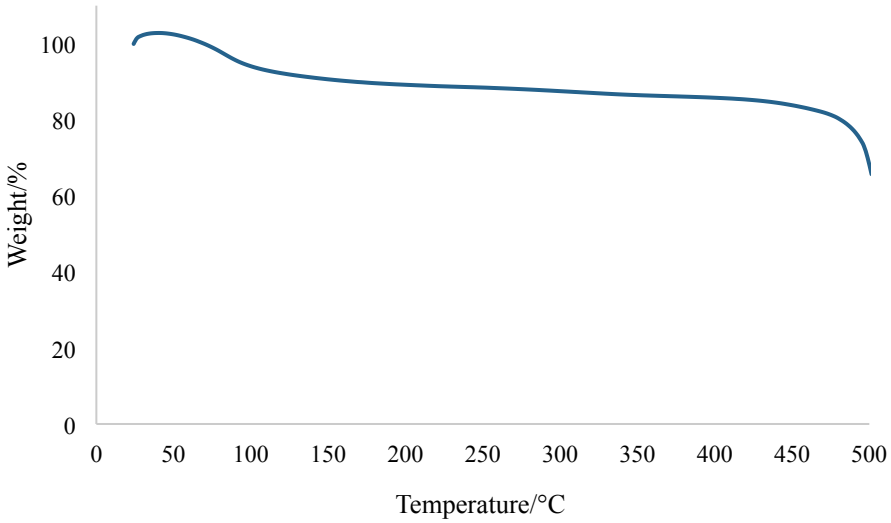

S3.2 – TGA results of MOF **2'**.

5. MOF washing regime further details

The activated samples used in the sensing of the explosive related compounds were generated through an implemented washing regime. The crystals present in the MOF **1** and **2** samples were initially dried under vacuum through the use of Buchner filtration. The resultant crystals were subsequently immersed in methanol for four days. After four days, the crystals were re-dried using Buchner filtration followed by immersion of the crystals in dichloromethane for 3 days. A final filtration of the crystals yielded the active materials used in sensing.

6. Extra sensing results and Fluorescence emission graphs used to produce quenching figures in paper.

Figure **S6.1** gives the fluorescence emission profiles of H_2dcbpy upon exposure to NB for varying amounts of time.

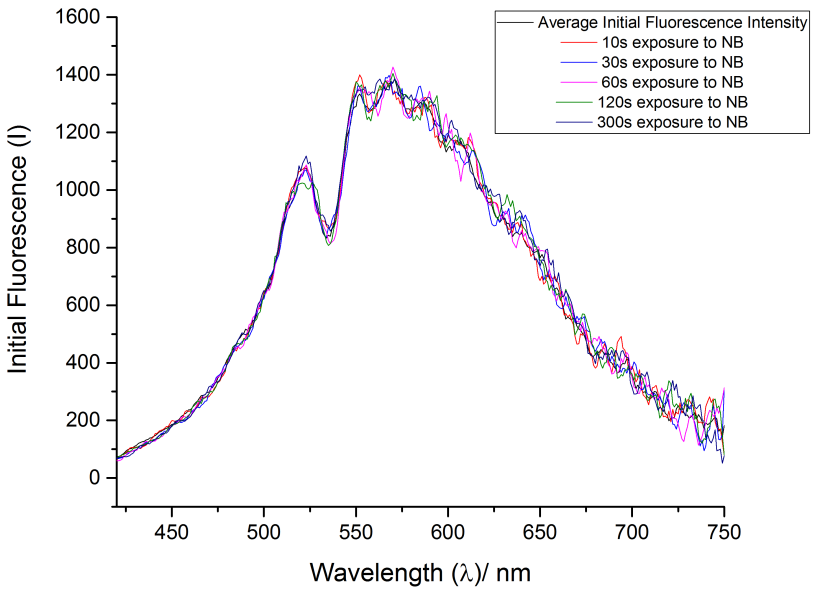

S6.1 - Fluorescence emission profile of the free linker ligand H_2dcbpy upon exposure to NB.

Figure 6.2 – Fluorescence emission profile of a representative MOF 1' thick film upon exposure to *p*-NT.

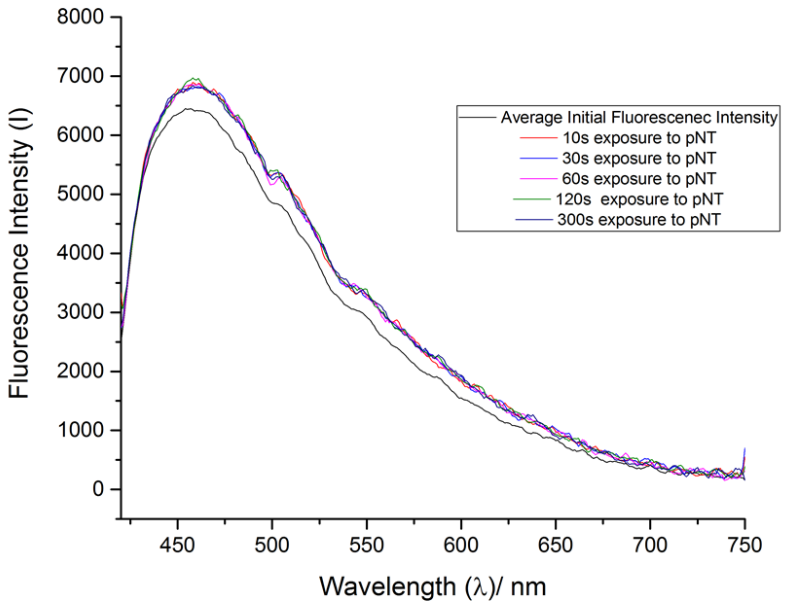

Figure 6.3 – Fluorescence emission profiles of MOF **1'** thin films upon exposure to analytes DMNB, NB, p-NT and 2,4-DNT.

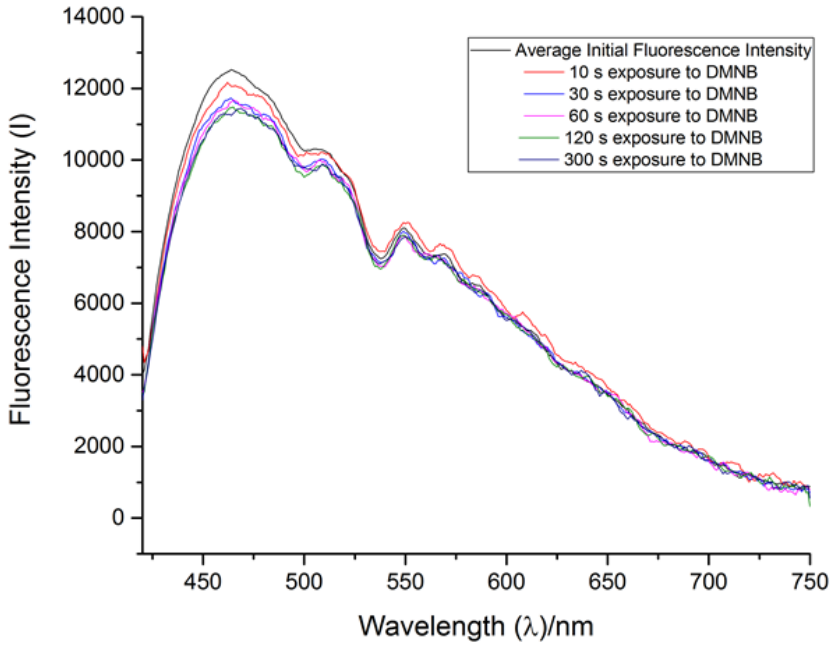

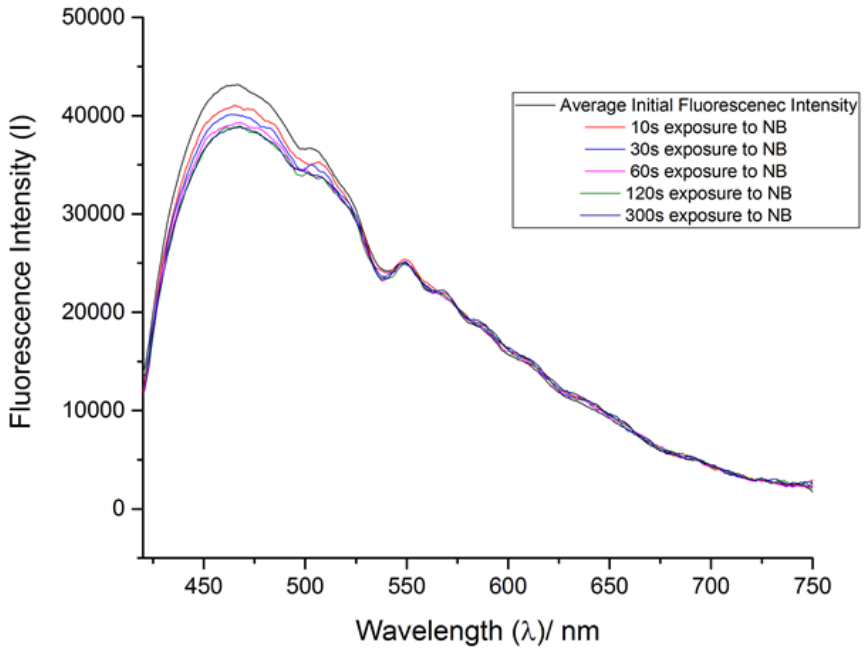

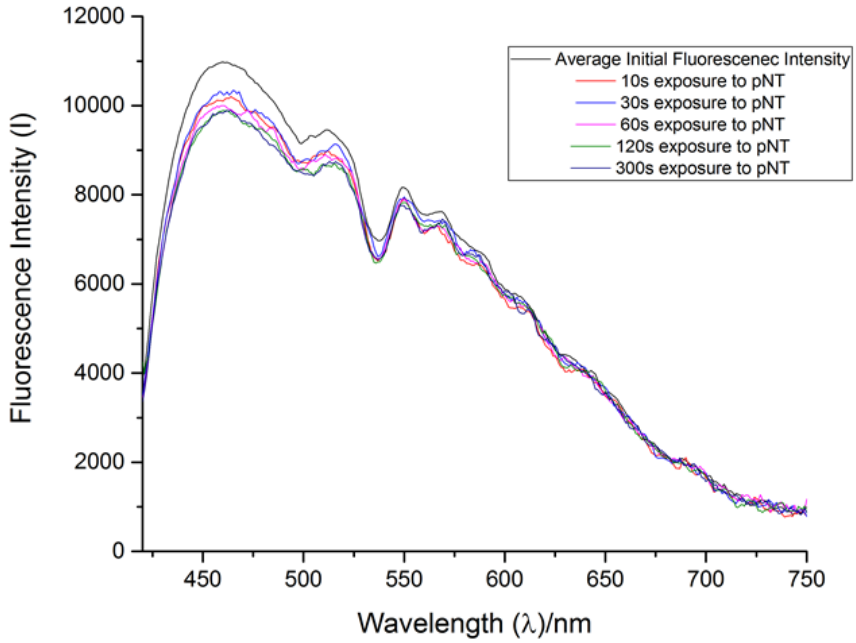
Average Initial Fluorescenec Intensity
10s exposure to pNT
30s exposure to pNT
60s exposure to pNT
120s exposure to pNT
300s exposure to pNT
Fluorescence Intensity (I)
Wavelength (λ)/nm
0
2000
4000
6000
8000
10000
12000
450
500
550
600
650
700
750

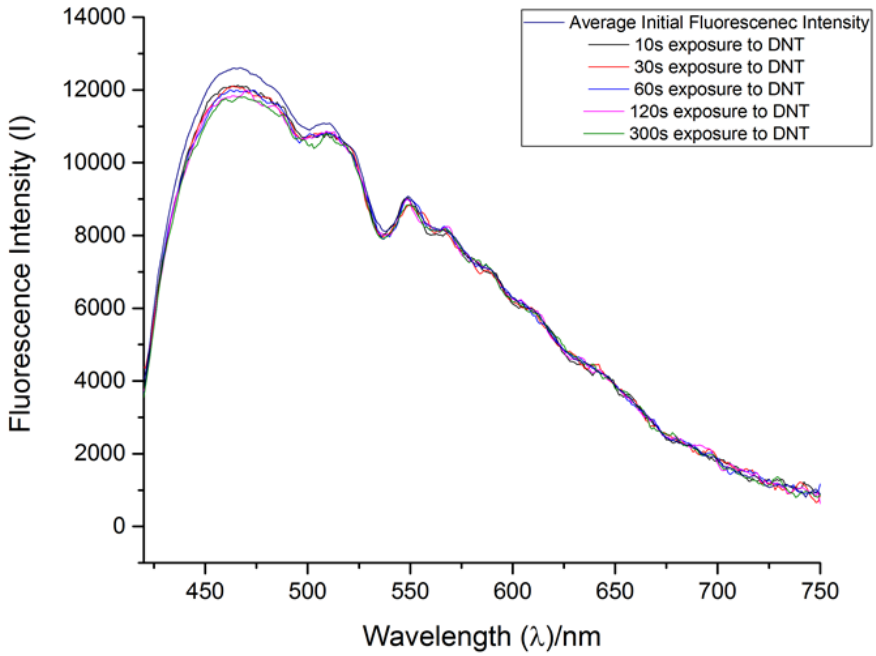
Average Initial Fluorescenec Intensity
10s exposure to DNT
30s exposure to DNT
60s exposure to DNT
120s exposure to DNT
300s exposure to DNT
Fluorescence Intensity (I)
Wavelength (λ)/nm
0
2000
4000
6000
8000
10000
12000
14000
450
500
550
600
650
700
750

Figure 6.4 – Fluorescence emission profiles of MOF **1M'** thin films upon exposure to analytes DMNB, NB, p-NT and 2,4-DNT.

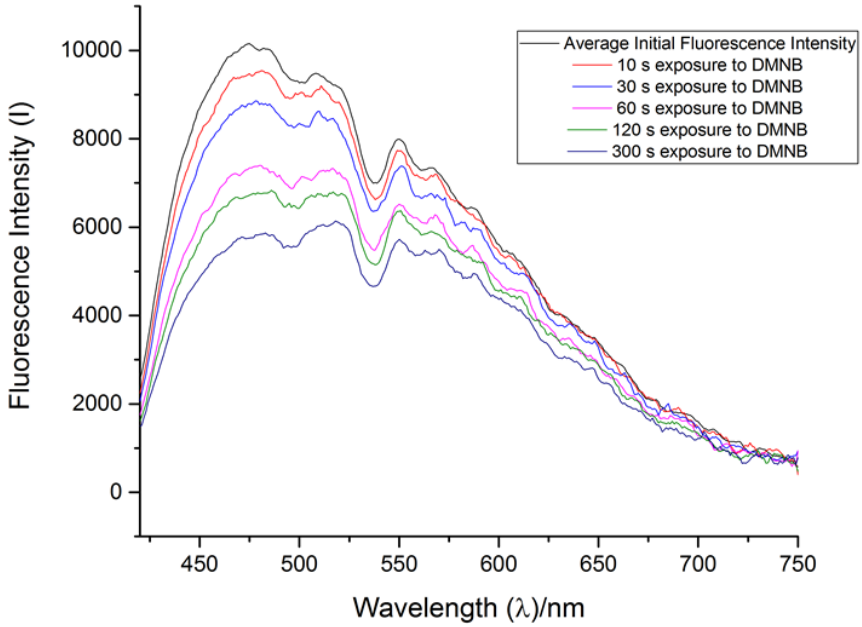

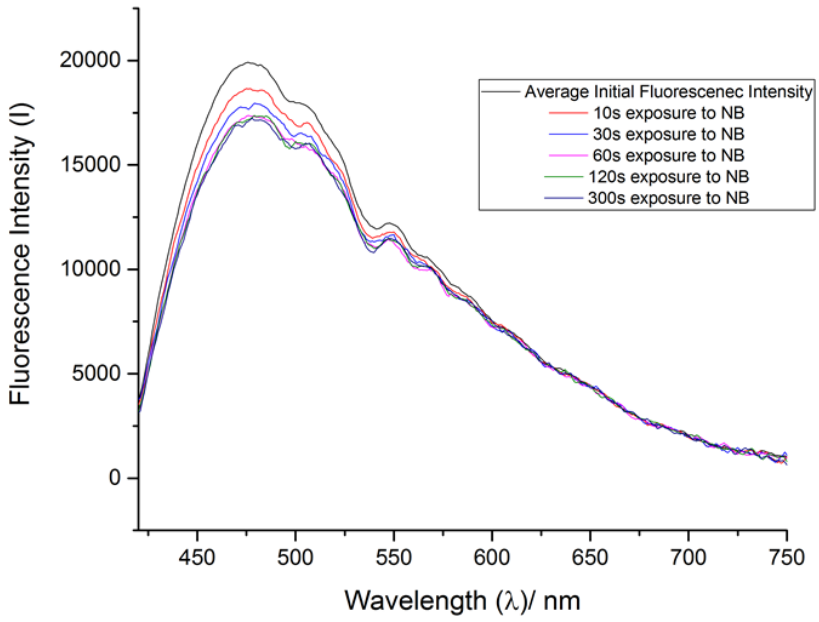

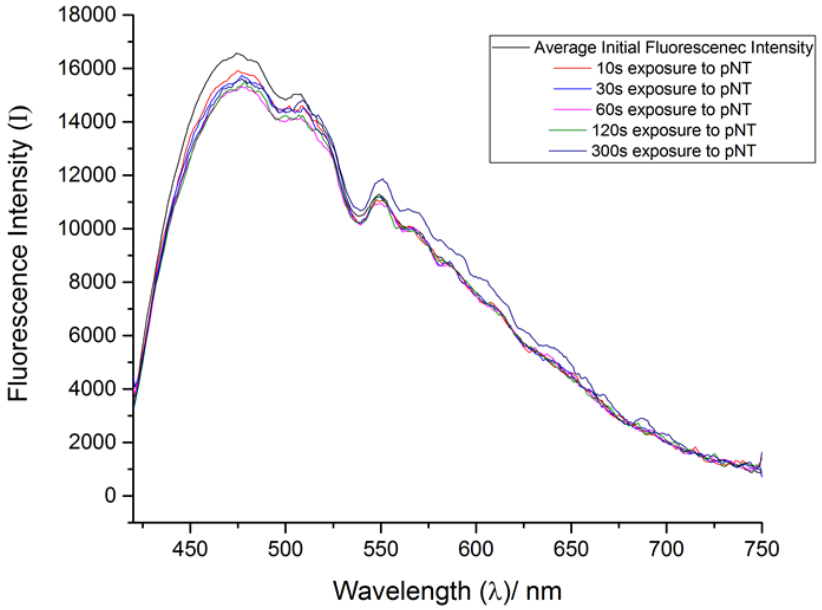
Average Initial Fluorescenec Intensity
10s exposure to pNT
30s exposure to pNT
60s exposure to pNT
120s exposure to pNT
300s exposure to pNT
Fluorescence Intensity (I)
Wavelength (λ)/ nm
18000
16000
14000
12000
10000
8000
6000
4000
2000
0
450
500
550
600
650
700
750

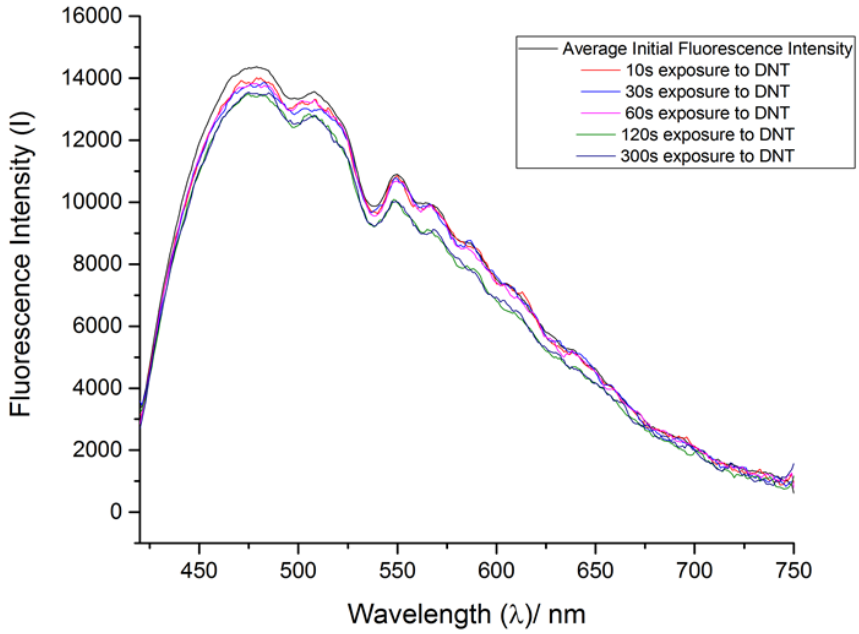
Average Initial Fluorescence Intensity
10s exposure to DNT
30s exposure to DNT
60s exposure to DNT
120s exposure to DNT
300s exposure to DNT
Fluorescence Intensity (I)
Wavelength (λ)/ nm
16000
14000
12000
10000
8000
6000
4000
2000
0
450
500
550
600
650
700
750

Figure 6.5 – Fluorescence emission profiles of MOF **2'** thin films upon exposure to analytes DMNB, NB, p-NT and 2,4-DNT.

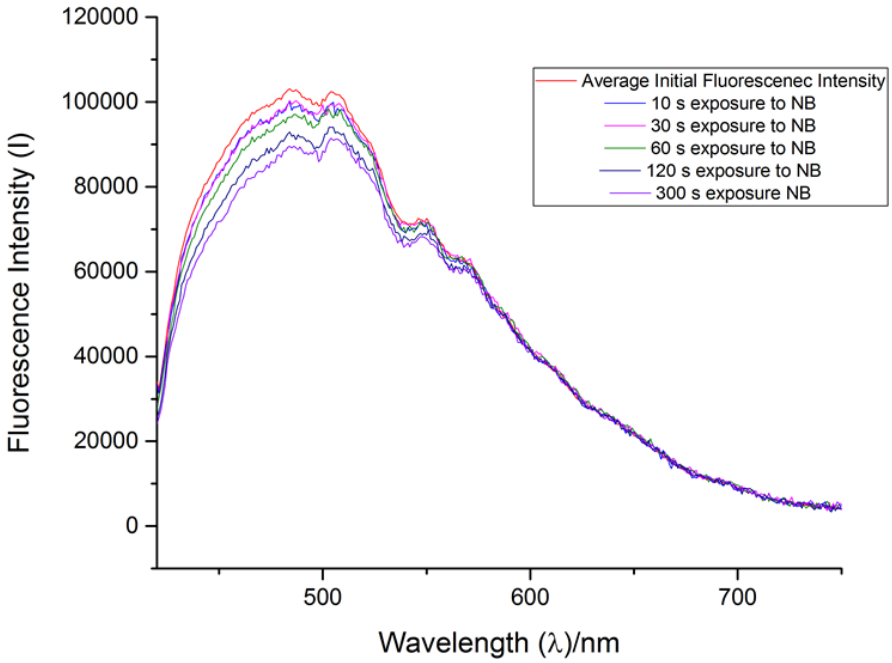

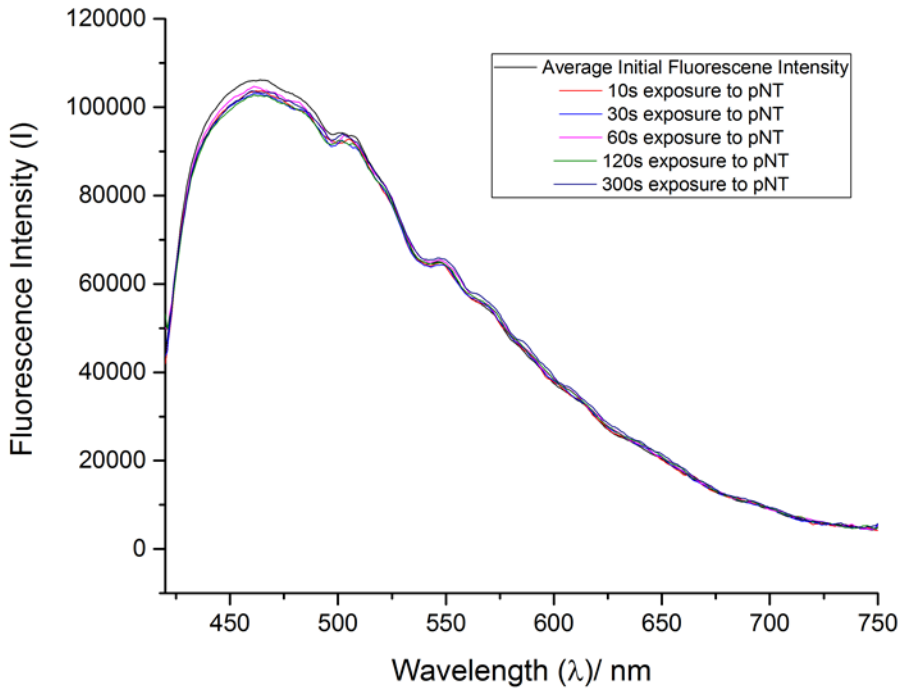

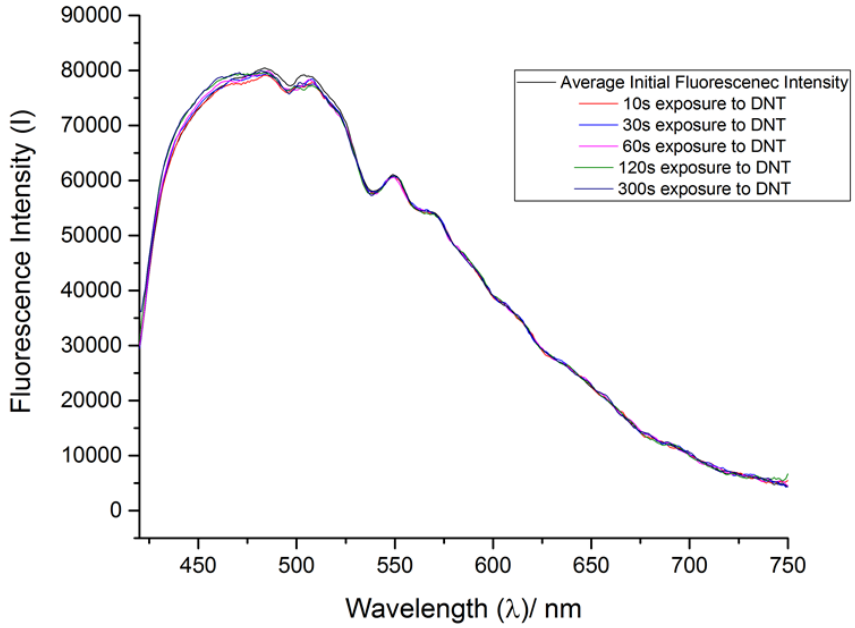
Average Initial Fluorescenec Intensity
10s exposure to DNT
30s exposure to DNT
60s exposure to DNT
120s exposure to DNT
300s exposure to DNT
Fluorescence Intensity (I)
Wavelength (λ)/ nm
90000
80000
70000
60000
50000
40000
30000
20000
10000
0
450
500
550
600
650
700
750

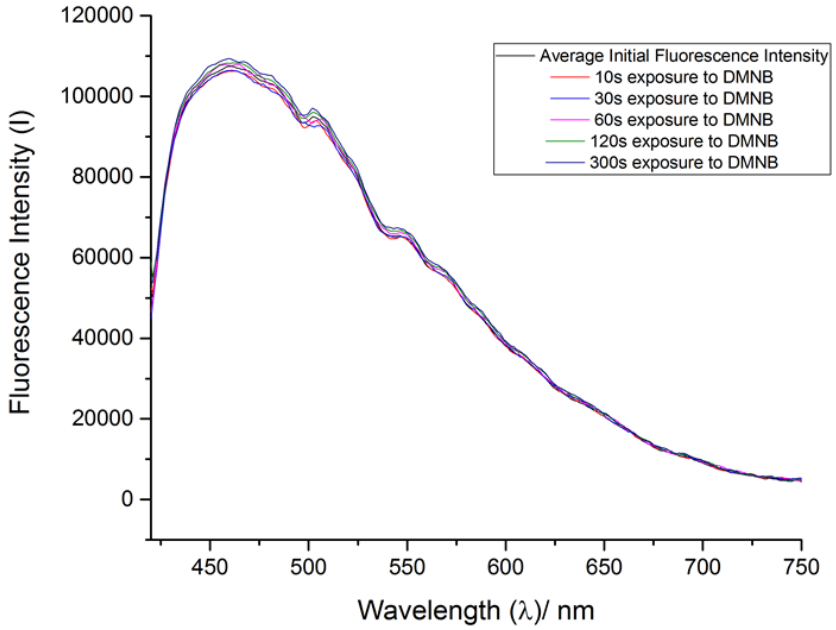
Average Initial Fluorescence Intensity
10s exposure to DMNB
30s exposure to DMNB
60s exposure to DMNB
120s exposure to DMNB
300s exposure to DMNB
Fluorescence Intensity (I)
Wavelength (λ)/ nm
120000
100000
80000
60000
40000
20000
0
450
500
550
600
650
700
750

7. Other examples of DMNB sensing

Significant sensing results for DMNB in vapour and solution phase in the literature. This work achieved 46.4% in 300 s. The exposure time or concentration of analyte is given where known.

Group/Reference	Solution or Vapour Phase	Sensitivity
Li et al.[1]	Vapour	84%, 10 s
Li et al.[2]	Vapour	8%, 15 min
Li et al.[3]	Vapour	< 10%, 10 min
Li et al.[4]	Vapour	47%
Ghosh et al.[5]	Vapour	57%, 5 min
Ghosh et al.[6]	Solution (H_2O)	< 10%
Cao et al.[7]	Solution (ethanol)	21% (200 ppm)

References

1. A. Lan, K. Li, H. Wu, D. H. Olson, T. J. Emge, W. Ki, M. Hong, and J. Li, *Angew. Chem. Int. Ed. Engl.*, 2009, **48**, 2334–2338.
2. S. Pramanik, C. Zheng, X. Zhang, T. J. Emge, and J. Li, *J. Am. Chem. Soc.*, 2011, **133**, 4153–4155.
3. D. Banerjee, Z. Hu, S. Pramanik, X. Zhang, H. Wang, and J. Li, *CrystEngComm*, 2013, **15**, 9745–9750.
4. Z. Hu, S. Pramanik, K. Tan, C. Zheng, W. Liu, X. Zhang, Y. J. Chabal, and J. Li, *Crystal Growth & Design*, 2013, **13**, 4204–4207.
5. A. K. Chaudhari, S. S. Nagarkar, B. Joarder, and S. K. Ghosh, *Crystal Growth & Design*, 2013, **13**, 3716–3721.
6. S. S. Nagarkar, A. V. Desai, and S. K. Ghosh, *Chem. Commun.*, 2014, **50**, 8915.
7. W.-J. Li, J. Lü, S.-Y. Gao, Q.-H. Li, and R. Cao, *J. Mater. Chem. A*, 2014, **2**, 19473–19478.

8. BET

BET measurements were attempted with N_2 on a Micromeritics Gemini VII 2390 Surface Area Analyzer instrument. A sample (approx. 80 mg) was outgassed at 200 °C for 24 hours, before analysis. Unfortunately N_2 proved adherent in the structure, leading to large underestimates of the surface area, and no isotherm for pore size calculations. MOF **1'** returned a value of 69.2857 m^2/g. This illustrates that the MOF is porous, but unfortunately leads to no information on pore size/volume.

9. Microwave details

The domestic microwave in which experiments were conducted was a Dunelm Mill P70B17EP-S4 microwave. With an input of 1200 W input (230-240 V, approx. 50 Hz) and an output of 700 W with a frequency of 2450 MHz, operating at 40% of the power output (280 W).

The three repeat experiments followed the same methodology as detailed in the experimental section of the paper. The PXRD patterns of the repeated experiments, are given along side the simulated PXRD of the [Zn(dcbpy)(DMF)]·DMF as obtained from crystallographic data. As is evident all of the PXRDs are in perfect accordance and thus demonstrating repeatability of results.